Materials Research Proceedings 37 (2023) 161-165 https://doi.org/10.21741/9781644902813-35

Pattern recognition of the flow around a pitching NACA 0012 airfoil in dynamic stall conditions

Giacomo Baldan[1,a *], Alberto Guardone[1,b]

[1]Department of Aerospace Science and Technology, Politecnico di Milano, Via La Masa 34, Milano 20156, Italy

[a]giacomo.baldan@polimi.it, [b]alberto.guardone@polimi.it

Keywords: Dynamic Stall, Proper Orthogonal Decomposition, Pitching Airfoil, Pattern Recognition, Helicopters, Wind Turbines

Abstract. The present work numerically investigates the flow evolution of a pitching NACA 0012 airfoil incurring in deep dynamic stall phenomena. The experimental data at Reynolds number Re = $1.35 \cdot 10^5$ and reduced frequency k = 0.1, provided by Lee et al., are compared to numerical simulation using different methods. Firstly, 2D URANS with different turbulence models are explored highlighting the advantages and the drawbacks of each strategy. On the one hand, simulations are able to describe most characteristic flow features of dynamic stall. On the other hand, numerical models still struggle in describing the inherent complexity of instability and transition from laminar to turbulence, resulting in a misprediction of the angle of attack at which the dynamic stall vortex (DSV) is generated and convected rearward. Finally, a Proper Orthogonal Decomposition (POD) is proposed to analyze the main flow features and to recognize flow patterns. The decomposition of both velocity magnitude and pressure fields shows a high frequency content requiring a large portion of the modes to recover most of the flow energy.

Introduction

Dynamic stall is a complex unsteady aerodynamic phenomenon that is present in a large range of engineering applications such as retreating blades of helicopter rotors, wind turbines, turbomachinery and maneuvering fixed wing aircraft [1]. Compared to static stall, it is characterized by a temporary delay of the boundary layer separation followed by a large flow detachment on the suction side of the profile. This results in a loss of lift, a strong pitch down moment, and an increase in drag. Before the flow reattachment, the profile underlays varying loads due to the chaotic nature of the involved phenomena.

Especially during the last decade, many experiments and computational simulations have been performed to further investigate dynamic stall phenomena and study the flow around pitching and plunging airfoils [2]. Low-fidelity tools are still unable to capture the main features of the flow and computational fluid dynamics should be leveraged [3]. Most difficulties rely in the modelling of the laminar separation bubble (LSB) and the subsequent creation of the dynamic stall vortex (DSV). Laminar to turbulent transition plays a major role in the formation and the convection of the DSV that influences a significant portion of the flow evolution.

In this paper, the flow around a pitching NACA 0012 profile underlying deep dynamic stall regime is numerically investigated. Firstly, a space and time convergence study is conducted using 2D RANS equations. Then, three different turbulent models are compared focusing on the LSB and DSV description. Finally, a Proper Orthogonal Decomposition (POD) is performed using the pressure and velocity magnitude fields.

Numerical setup

The numerical setup aims at reproducing the experimental campaign presented in Lee et al. [4]. A NACA 0012 profile with c=0.15 m chord underlying a sinusoidal pitching motion, at reduced

Content from this work may be used under the terms of the Creative Commons Attribution 3.0 license. Any further distribution of this work must maintain attribution to the author(s) and the title of the work, journal citation and DOI. Published under license by Materials Research Forum LLC.

Materials Research Proceedings 37 (2023) 161-165 https://doi.org/10.21741/9781644902813-35

frequency k=0.1 ($k=\omega \cdot c/2 / V_\infty$) and Reynolds number $Re = 1.35 \cdot 10^5$, is investigated. The free-stream velocity is $V_\infty = 14$ m/s with a turbulent intensity equal to 0.08%, pressure is $P_\infty = 1$ atm, and the pitching frequency ω is set equal to 18.67 Hz. Three different O-grids have been generated as reported in Tab. 1, where N_x is the number of points around the profile and N_y in the normal direction. All grids respect the $y^+ < 1$ requirement at the wall.

Table 1: NACA 0012 O-grid specifications

O-Grids	N_x	N_y	Δx_{le} ($\cdot 10^{-3}$c)	Δx_{te} ($\cdot 10^{-4}$c)
G1	384	96	3.3	8.4
G2	512	128	2.0	5.0
G3	1024	256	0.67	3.6

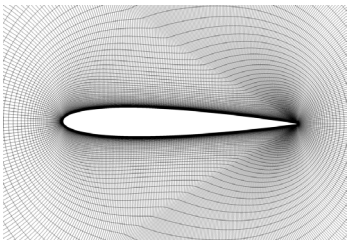

Figure 1: O-grid detail

Numerical simulations are performed using ANSYS Fluent 2023R1. The unsteady incompressible RANS equations are solved using second-order upwind discretization and second-order implicit time integration scheme. Gradients are retrieved through a least square cell-based method and fluxes are obtained with the Rhie-Chow momentum-based formulation. Pressure-velocity equations are solved using the SIMPLE method. A rigid motion of the entire grid is prescribed to allow the airfoil pitching, $\alpha(t) = 10° + 15° \sin(\omega t)$.

The POD decomposition is chosen, in this work, because it is the linear decomposition that, on average, minimize the energy loss considering a subset of *k* modes and it also grants the orthogonality of the modes [5]. The POD is computed using the Singular Value Decomposition (SVD) method.

Results

As a first step, time and grid independence study is performed. For each mesh three different simulations have been computed using 900, 1800, and 3600 time steps per pitching cycle. SST model with intermittency equation close the RANS equations system. All simulations are run until the solution of subsequent cycles overlaps, usually requiring three or four cycles. In Fig. 2 the last converged cycle is reported. The convergence has to be mainly verified in the upstroke part and on the angle at which the DSV generates the peak in lift and drag. All three grids show a good agreement in the aforementioned points but G1 should not be used since the low resolution does not satisfactory describe the DSV evolution, resulting in a larger mismatch in the downstroke part.

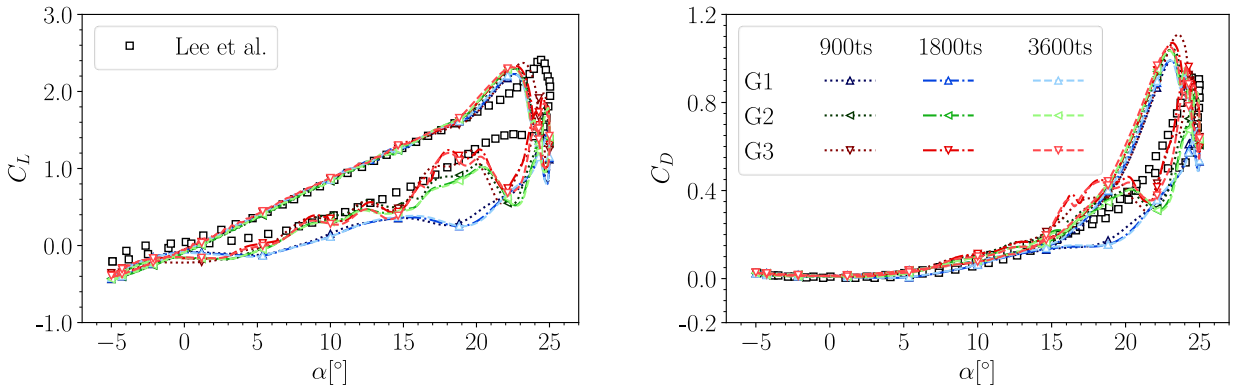

Figure 2: Space and time convergence study. Experimental data [4].

Materials Research Proceedings 37 (2023) 161-165 https://doi.org/10.21741/9781644902813-35

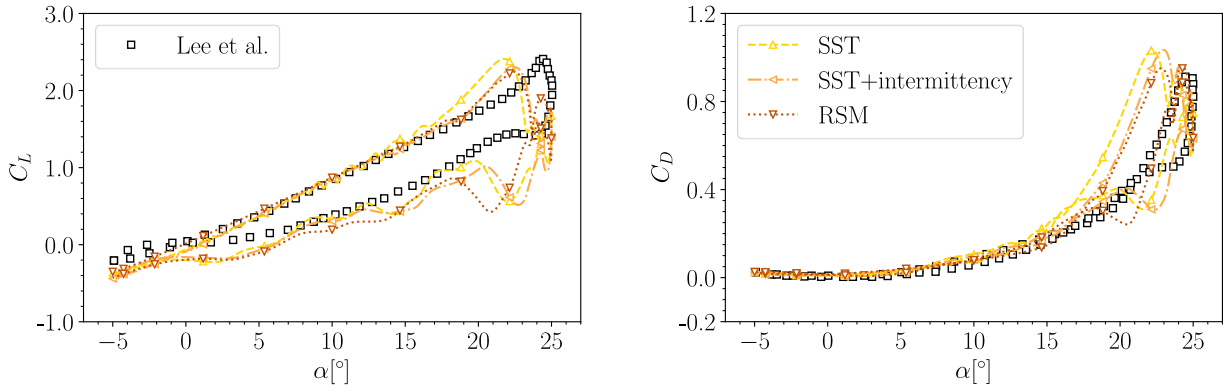

Figure 3: Turbulence model comparison using G2 grid and 3600 time steps per cycle. Experimental data [4].

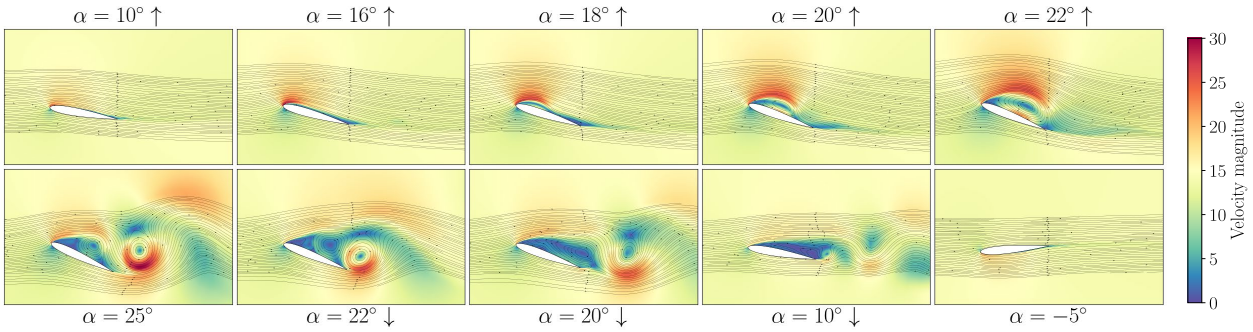

Figure 4: Velocity magnitude contours and streamlines at different pitch angles.

Another critical aspect in dynamic stall simulations is turbulence modelling. SST, SST with intermittency equation, and RSM models are tested using the G2 grid and 3600 time steps per cycle. In Fig. 3, it can be noted that standard SST model fails to describe the LSB and results in oscillation in the DSV formation. The same behavior is present in the RSM even if the effect is weaker since the individual components of the Reynolds stress tensor are computed. The SST model coupled with the intermittency equation describes in more detail the transition from laminar to turbulent giving more accurate results. For this last case, the velocity magnitude contour and streamlines are reported in Fig. 4 to represent the dynamic stall phenomena.

Finally, the POD decomposition is computed for pressure and velocity magnitude fields in the airfoil reference frame during an entire cycle. In Fig. 5 the eigenvalues are shown while in Fig. 6 the first ten modes are represented. The first mode, which is the most energetic one, represent the mean flow over the entire cycle. The following modes confirm the crucial role of the DSV evolution. As the number of the mode increases higher frequency content is represented. It is visible how the DSV that detaches from the leading edge interacts with the stall that originates from the trailing edge. The high frequency content of the flow is confirmed by the cumulative eigenvalue spectrum in which the number of modes required to represent 99% of the energy are 155 and 503 for pressure and velocity, respectively.

Conclusion

In this work, a pitching NACA 0012 underlying dynamic stall phenomena is investigated using 2D URANS with three turbulence models. Numerical simulations are able to describe the LSB and the DSV, showing a good agreement with experiments in the upstroke phase but are not able to capture the angle at which the DSV is convected rearwards anticipating the drag and lift picks. The LSB is shown to play a crucial role in the flow evolution requiring a turbulence model capable of describing the transition from laminar to turbulent, as in the case of SST with intermittency

equation. In addition, a POD is provided for both pressure and velocity magnitude fields to extract the main flow features and to emphasize the interactions of leading and trailing edge stall.

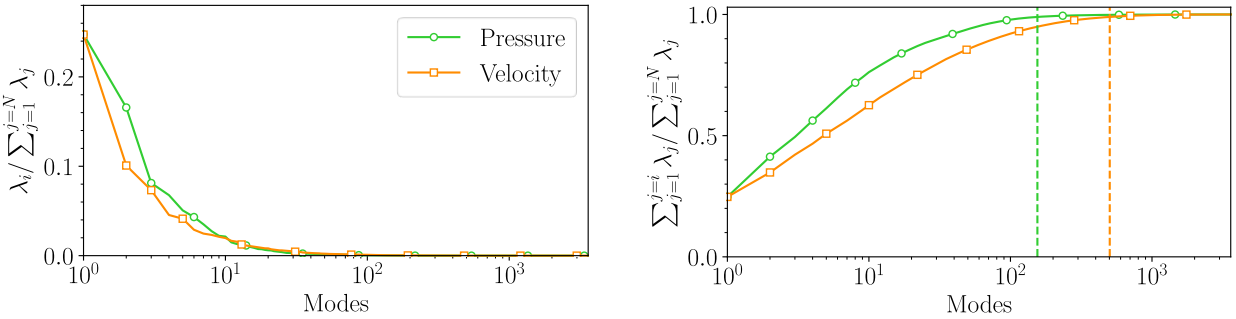

Figure 5: Pressure and velocity magnitude POD eigenvalues and cumulative eigenvalue spectrum. The dashed lines show the number of modes required to represent 99% of the energy.

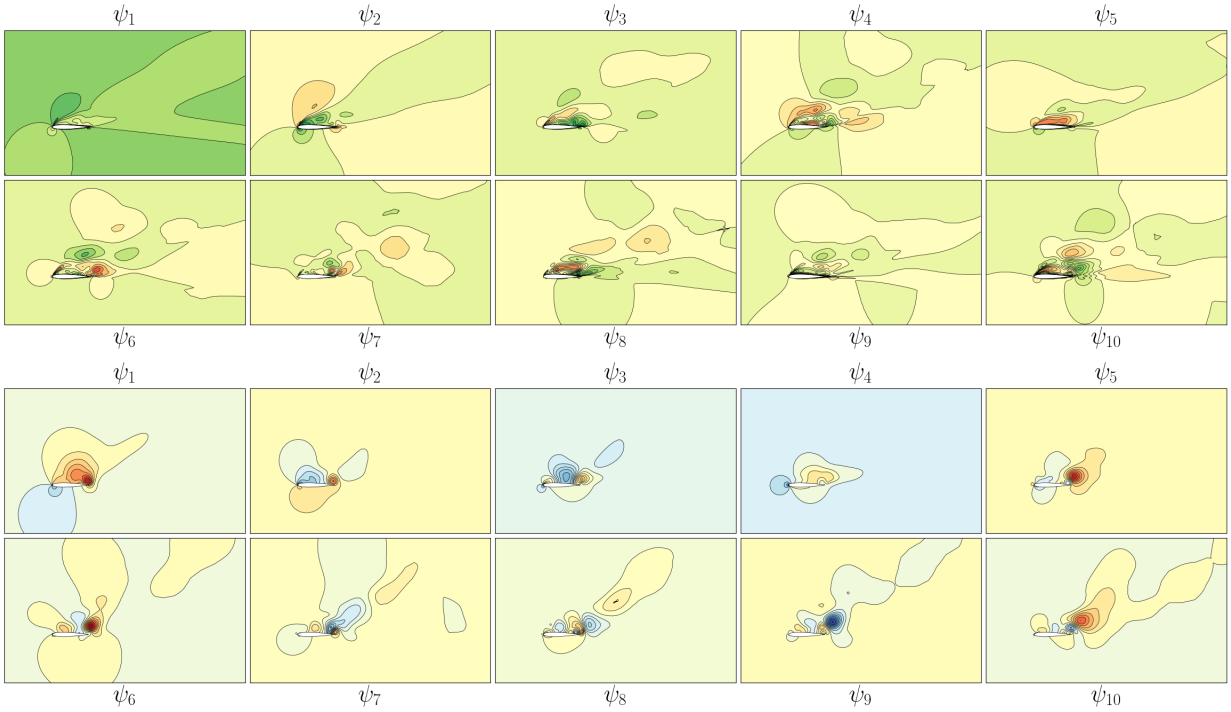

Figure 6: First ten POD modes of velocity magnitude (above) and pressure (below) fields.

References

[1] M. Visbal, D. Garmann, "Analysis of Dynamic Stall on a Pitching Airfoil Using High-Fidelity Large-Eddy Simulations". AIAA Journal 2018; 56(1):46-63. https://doi.org/10.2514/1.J056108

[2] F. Avanzi, F. de Vanna, Y. Ruan and E. Benini, "Enhanced Identification of Coherent Structures in the Flow Evolution of a Pitching Wing". AIAA 2022-0182. AIAA SCITECH 2022 Forum. https://doi.org/10.2514/6.2022-0182

[3] A. D. Gardner, A. R. Jones, K. Mulleners, J. W. Naughton, M. J. Smith. "Review of rotating wing dynamic stall: Experiments and flow control". Progress in Aerospace Sciences 2023; 137:100887. https://doi.org/10.1016/j.paerosci.2023.100887

[4] T. Lee, P. Gerontakos, "Investigation of flow over an oscillating airfoil". Journal of Fluid Mechanics 2004; 512:313–341. https://doi.org/10.1017/S0022112004009851

[5] H. Eivazi, S. Le Clainche, S. Hoyas, R. Vinuesa. "Towards extraction of orthogonal and parsimonious non-linear modes from turbulent flows". Expert Systems with Applications 2022; 202:117038. https://doi.org/10.1016/j.eswa.2022.117038